Mechanics Research Communications 65 (2015) 24–29

Contents lists available at ScienceDirect

Mechanics Research Communications

journal homepage: www.elsevier.com/locate/mechrescom

Breaking bore: Physical observations of roller characteristics

Xinqian Leng, Hubert Chanson*

The University of Queensland, School of Civil Engineering, Brisbane, QLD 4072, Australia

ARTICLE INFO

Article history:
Received 28 October 2014
Received in revised form 20 February 2015
Accepted 21 February 2015
Available online 28 February 2015

Keywords:
Bore roller
Compression waves
Open channels
Free-surface profile
Roller shape
Roller toe perimeter
Bore celerity
Hydraulic jump

ABSTRACT

In an estuary, a tidal bore is a hydraulic jump in translation generated at the leading edge of the flood tide during the early flood tide under spring macrotidal conditions in a narrow funnelled channel. After formation, the bore is traditionally analysed as a hydraulic jump in translation and its leading edge is characterised by a breaking roller for $Fr_1 > 1.3$–1.5. Herein new unsteady experiments were conducted to investigate in details the upstream propagation of breaking bore roller. The toe perimeter shape fluctuated rapidly with transverse distance and time. A characteristic transverse wave length of the toe perimeter was observed. Both the standard deviation of toe perimeter location and characteristic transverse wave length were comparable to field observations. The celerity of the roller toe fluctuated rapidly with time and space. The instantaneous longitudinal profile of the roller free-surface showed significant temporal and spatial fluctuations. Although the bore propagation may be analysed in an integral form in first approximation, the rapid fluctuations in roller toe perimeter and free-surface profiles indicated a strongly three-dimensional turbulent flow motion.

1. Presentation

A tidal bore is the leading edge of the flood tide in a funnel shaped river mouth under macro-tidal conditions, associated with a discontinuity of the free-surface (Fig. 1). It is an unsteady, rapidly varied and highly turbulent open channel flow [1–3]. Several studies demonstrated the impact of tidal bores in sediment processes [4,5]. A related process is the tsunami-induced bore propagating upriver surge [6]. When the difference in flow depths across the tidal bore is large, the bore is characterised by a breaking roller as seen in Fig. 1A [1,7]. The roller toe is a flow singularity where air is entrapped and vorticity is generated [8].

In the present study, the upstream propagation and shape of breaking bores are investigated experimentally. It is shown that, although the bore celerity and roller shape are assumed quasi-uniform in traditional theoretical developments, the roller toe propagation is a highly turbulent process. Its properties are developed, and physical observations are discussed.

2. Theoretical background

The driving process of a tidal bore is a large tidal range which may be locally amplified by a number of factors: for example, when the natural resonance period of the estuary is close to the tidal period. When the sea level rises with time during the early flood tide, the tidal wave steepness increases with distance from the river mouth until the leading edge of the tidal wave becomes an abrupt front: that is, the tidal bore. After formation, the tidal bore is characterised by an abrupt rise in water depth (Fig. 1), and the bore front may be analysed as a hydraulic jump in translation [2,9]. In a system of reference in translation with the bore, the integral form of the continuity and momentum equations gives:

$$(V_1 + U)A_1 = (V_2 + U)A_2 \tag{1}$$

$$\rho(V_1 + U)A_1((V_1 + U) - (V_2 + U)) = \int\int_{A_2} P \; dA - \int\int_{A_1} P \; dA + F_{fric} - W \sin\theta \tag{2}$$

where V is the flow velocity positive downstream, U the bore celerity positive upstream, ρ the water density, g the gravity acceleration, A the channel cross-sectional area measured perpendicular to the flow direction, P the pressure, F_{fric} the flow resistance force, W the weight force, θ the angle between the bed slope and horizontal, and the subscripts 1 and 2 refer to the flow conditions immediately before and after the bore respectively (Fig. 1B).

In presence of some flow resistance and bed slope effect, the continuity and momentum principles yield to a relationship between

* Corresponding author. Tel.: +61 7 3365 3516; fax: +61 7 3365 4599.
E-mail address: h.chanson@uq.edu.au (H. Chanson).

http://dx.doi.org/10.1016/j.mechrescom.2015.02.008
0093-6413/

(A)

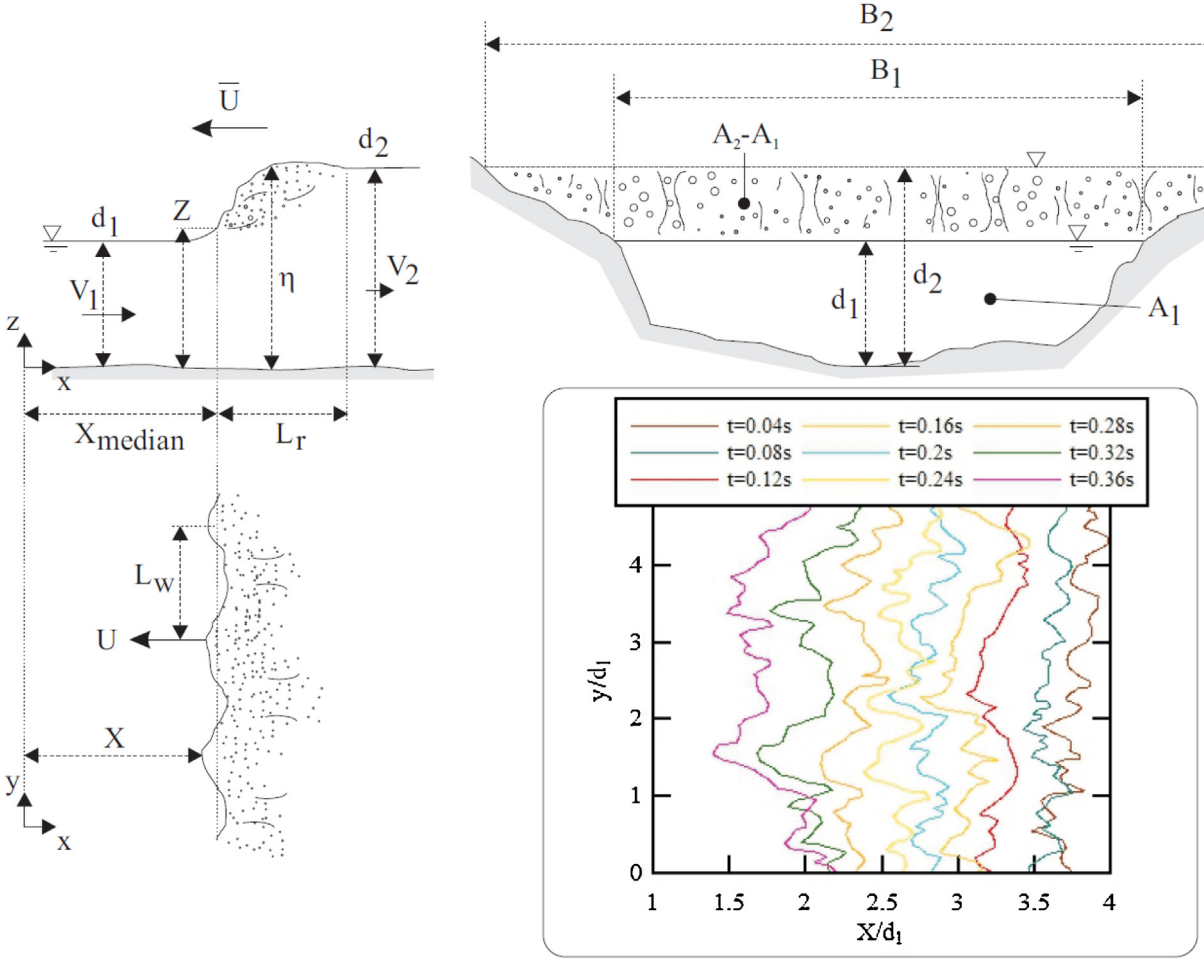

(B)

Fig. 1. Breaking tidal bore propagation. (A) Looking downstream at the Qiantang River bore in the northern channel downstream of Xinchang, China on 6 September 2013 at 11:50 – $d_1 \sim 1$ m, $\bar{U} \sim 3.6$ m/s, $Fr_1 \sim 2.1$. (B) Definition sketch – bottom left Inset: Instantaneous roller toe perimeter as function of time (Run 2)

the conjugate cross-section area ratio A_2/A_1 and Froude number Fr_1:

$$Fr_1^2 = \frac{1}{2}\frac{A_2}{A_1}\frac{B_1}{B}\left(\left(2-\frac{B'}{B}\right)+\frac{B'}{B}\frac{A_2}{A_1}\right)+\frac{A_2}{A_2-A_1}\frac{F_{fric}-WS_o}{\rho g(A_1^2/B)} \quad (3)$$

where Fr_1 is the tidal bore Froude number:

$$Fr_1 = \frac{U+V_1}{\sqrt{g(A_1/B_1)}} \quad (4)$$

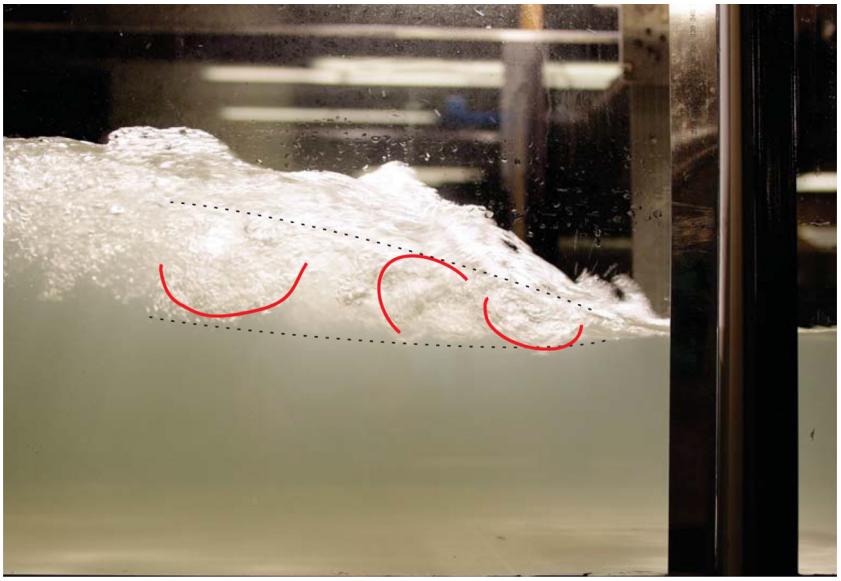

Fig. 2. Side view of coherent vortical structures in the shear layer of a roller – $Fr_1 = 1.65$, $Q = 0.085\ m^3/s$, shutter speed: 1/125 s, bore propagation from left to right.

In Eq. (3), B and B' are characteristic widths linked to the channel shape:

$$B = \frac{A_2 - A_1}{d_2 - d_1} \tag{5}$$

$$B' = \frac{\int_{A_1}^{A_2} \int \rho g (d_2 - y) dA}{\frac{1}{2}\rho g (d_2 - d_1)^2} \tag{6}$$

with d the flow depth (Fig. 1B). The theoretical result (Eq. (3)) implies a smaller ratio of conjugate depths d_2/d_1 with increasing flow resistance for a given bed slope, while the ratio of conjugate depths d_2/d_1 increases with increasing bed slope for a given flow resistance. The effects of flow resistance and bed slope decrease however with increasing Froude number, becoming negligible for Froude numbers greater than 2–3.

Neglecting the flow resistance, the result may be simplified for a horizontal channel into [10]:

$$\frac{A_2}{A_1} = \frac{1}{2} \times \frac{\sqrt{\left(2 - \frac{B'}{B}\right)^2 + 8\frac{(B'/B)}{(B_1/B)}Fr_1^2} - \left(2 - \frac{B'}{B}\right)}{(B'/B)} \tag{7}$$

For a tidal bore propagating in a smooth sloping rectangular prismatic channel, the combination of the continuity and momentum principles gives a physically meaningful solution assuming $\cos\theta \approx 1$, where θ is the angle between the bed slope and horizontal, positive for a channel sloping downwards in the downstream direction. Namely the ratio of conjugate depths equals:

$$\frac{d_2}{d_1} = \frac{1}{2}\left(\sqrt{(1-\varepsilon)^2 + 8\frac{Fr_1^2}{1-\varepsilon}} - (1-\varepsilon)\right) \tag{8}$$

where ε is a dimensionless coefficient defined as

$$\varepsilon = \frac{W\ \ S_o}{\rho g B_1 d_1^2 (Fr_1^2 - 1)} \tag{9}$$

with B_1 the channel width.

For a smooth horizontal rectangular prismatic channel, Eqs. (3), (7) and (8) yield to the Bélanger equation:

$$\frac{d_2}{d_1} = \frac{1}{2}\left(\sqrt{1 + 8Fr_1^2} - 1\right) \quad \text{Smooth horizontal rectangular channel} \tag{10}$$

The above integral approach assumes implicitly that the bore celerity is uniform and the roller shape is two-dimensional. Field and laboratory observations suggested that these assumptions are simplistic.

3. Physical study

The laboratory experiments were performed in a 19 m long 0.7 m wide horizontal channel, made of smooth PVC bed and 0.60 m high glass sidewalls. The experimental flow conditions are summarised in Table 1 where Q is the initial water discharge. The waters were fed by an intake structure, in which the inflow was streamlined before entering a smooth convergent leading to the 19 m long test section. A fast closing gate was located at the channel's downstream end ($x_{Gate} = 18.1$ m) where x is measured from the test section's upstream end. Video observations were performed using a HD video camera Sony™ HDR-XR160, operating at 25 fps or 50 fps, and a digital camera Casio™ Exlim EX-10, set at 120 fps, 240 fps or 480 fps. The video camera was mounted vertically looking down across the channel width. Photographs in high-speed continuously shooting mode (8.3 fps) were taken through the sidewalls during the bore front passage, using a dSLR Pentax™ K-3 with Carl Zeiss™ Distagon 28 mm f2 lens, producing photographs with a low degree (<1%) of barrel distortion. For all experiments, the discharge was $0.085\ m^3/s$. The breaking bore was generated by the complete fast closure of the Tainter gate and the bore propagated upstream against the initially steady flow (Table 1).

Laboratory data were compared with properties of the Qiantang River bore observed in the northern channel near Xinchang (China). On 6 September 2013, the bore roller was nearly straight and over 200 m wide, as it advanced towards the photographer (Fig. 1A). A number of dSLR photographs were recorded with a dSLR camera Pentax™ K-7 equipped with Voigtlander™ Nokton 58 mm f1.4 lens, and the analysed data are presented in terms of the roller toe perimeter.

4. Results

With breaking bores, air bubbles are entrapped at the roller toe that is a singularity (Figs. 1 and 2). The air entrainment is localised at the roller toe perimeter which is also a line source of vorticity, and a shear layer develops in the wake of the toe. Fig. 2 presents

Table 1
Physical investigation of breaking bores.

Reference	Run	Q (m^3/s)	V_1 (m/s)	d_1 (m)	$\bar{U}$ (m/s)	Fr_1	Instrumentation
Laboratory study	1	0.085	0.76	0.160	0.99	1.40	Video (25 fps) & photographs
	2	0.085	0.83	0.146	0.95	1.49	Video (50 fps) & photographs
	3	0.085	0.74	0.165	0.90	1.33	Video (120, 240, 480 fps)
Qiantang River bore	130906	–	–	~1	~3.6	~2.1	dSLR photography

Notes: d_1: initial water depth; Fr_1: bore Froude number; $\bar{U}$: cross-sectional time-averaged bore celerity; V_1: initial flow velocity.

a sideview of an advancing breaking bore, highlighting the large scale turbulent structures with horizontal transverse axis. As the coherent vortical structures are advected in the shear layer, they grow up in size by vortex pairing, as seen in stationary hydraulic jumps [11,12].

While the roller toe perimeter is assumed ideally straight, its instantaneous shape was wavy as illustrated in Fig. 1. The instantaneous perimeter data showed the broad range of instantaneous shapes of the roller toe perimeter. Fig. 1B (Inset) shows some instantaneous transverse profile, where $x = X$ is the instantaneous toe location at a transverse distance y, with $y = 0$ at the left side wall. The roller toe perimeter was quasi two-dimensional on average, but the data showed some occasional backshifts of roller toe location with time, implying some instantaneous, local negative celerity. The deviations of the roller toe perimeter about the instantaneous cross-sectional median position X_{median} indicated some quasi-periodic fluctuation of the toe perimeter across the section. Typical probability distribution functions of transverse perimeter fluctuation $(X - X_{median})$ are shown in Fig. 3A. The data sets exhibited a quasi-normal distribution, yielding $(X - X_{median})'/d_1 = 0.145$ on average at a given time. The pseudo-periodic shape of the roller toe perimeter implied the existence of non-linear structures, streamwise vortices and streaks, somehow similar to those observed in plane mixing layers and wall jets [13,14]. The existence of streamwise structures was complementary to the occurrence of organised structures in the shear layer seen in Fig. 2. At a fixed time, the transverse fluctuations of toe perimeter location around its median were analysed in terms of relevant transverse wave lengths L_w. For the laboratory data sets, the predominant transverse wave length was $L_w \sim 0.2$ m (i.e. $L_w/d_1 \sim 1.2$).

For comparison, the Qiantang River bore data yielded a dimensionless standard deviation $(X - X_{median})'/d_1$ was about 0.13, close to the present laboratory observations (Fig. 3B). In the Qiantang River, the transverse variation of instantaneous toe perimeter presented some pseudo-periodic fluctuations, with a range of wave lengths within $0.7 < L_w/d_1 < 25$, the two dominant dimensionless wave length ranges being $L_w/d_1 \sim 1$ and 5–10.

In laboratory, the instantaneous longitudinal profiles of roller free-surface highlighted the rapid fluctuations in roller surface's vertical elevations as well as the rapid changes in longitudinal roller profiles with time. The data indicated a maximum in free-surface fluctuations in the first half of the roller, as previously reported in stationary hydraulic jumps [15,16]. Visual observations showed that the free-surface elevation rose first slowly immediately prior to the roller, for Froude numbers less than 2, as sketched in Fig. 1B. The upward streamline curvature derived from theoretical considerations, namely the integral balances of linear momentum, in both horizontal and vertical directions, and of angular momentum [21] and was previously observed experimentally [8,17]. Data in terms of vertical elevation Z of the roller toe are presented in Fig. 4, in which they were compared with re-analysed breaking bore data [18,19]. Fig. 4A shows probability distributions of toe elevation about its median. Fig. 4B presents the dimensionless median toe elevation Z_{median}/d_1 and toe elevation fluctuations $(Z_{75}\text{-}Z_{25})/d_1$ data as functions of the Froude number, where Z_{75} and Z_{25} are the third and first quartiles respectively. All the data indicated a decrease in roller toe elevation, and in fluctuations in vertical elevation of roller toe, with increasing Froude number (Fig. 4B). The asymptotic limits presented two distinct trends. For $Fr_1 < 1.3$, the bore became undular and the roller disappeared. For $Fr_1 > 2$, the dimensionless roller toe elevation Z/d_1 tended to unity and the fluctuations in roller toe elevation tended to small values equal to the initial free-surface fluctuations.

5. Discussion

The bore roller celerity was calculated based upon the instantaneous roller toe positions. The channel width was divided into seven 0.1 m wide sub-sections, and the mean celerity of each individual sub-section was estimated as a function of time. Statistical

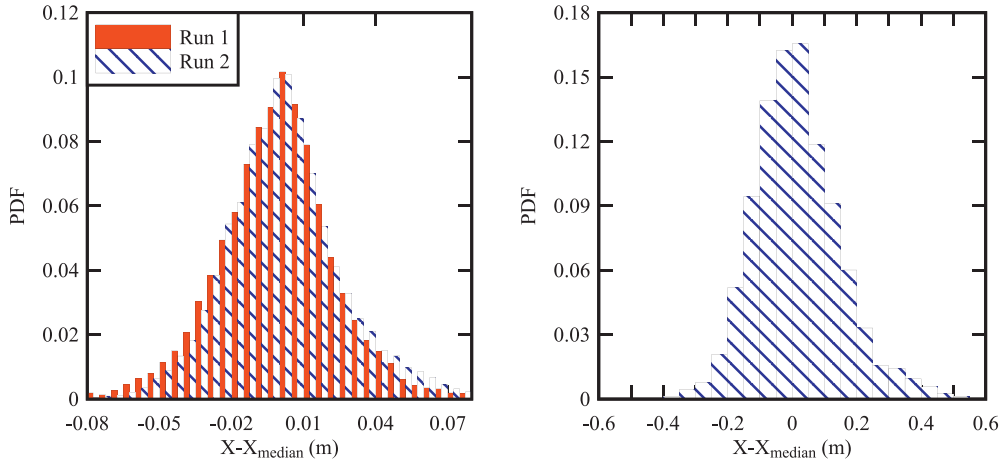

Fig. 3. Probability distribution function of longitudinal fluctuations in roller toe perimeter about the median – Left: laboratory data; Right: field data.

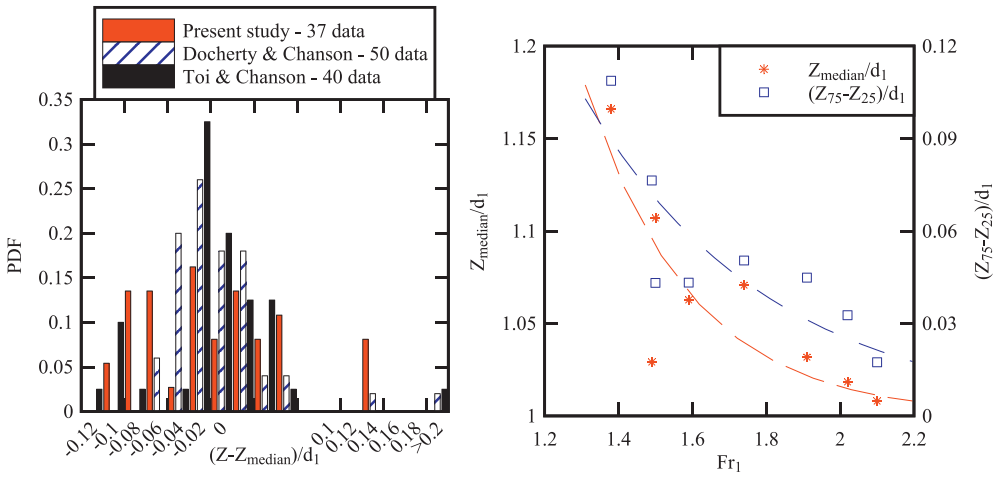

Fig. 4. Vertical elevation Z/d_1 of roller toe – Left: probability distribution function of roller toe elevation about the median; Right: median elevation and difference between third and first quartiles – comparison between laboratory data.

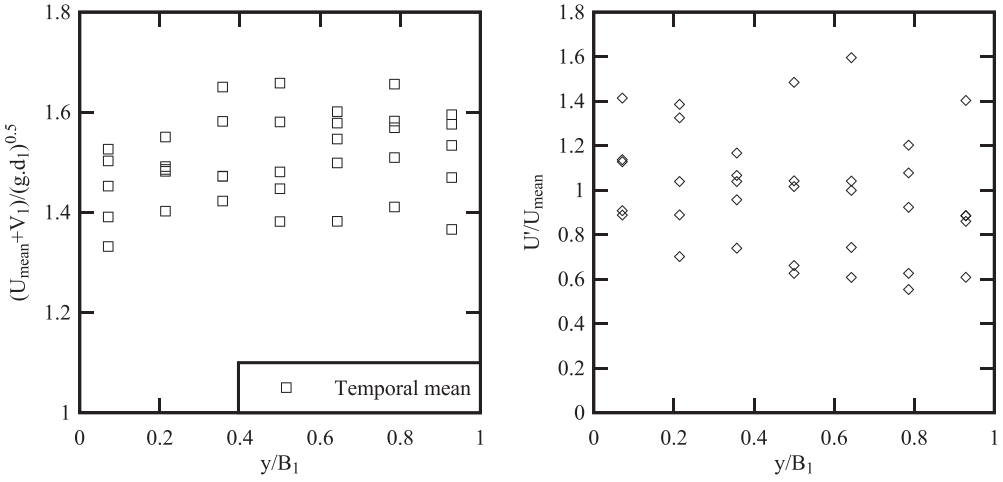

Fig. 5. Transverse variation in roller toe celerity and celerity fluctuations – Left: temporal mean celerity; Right: standard deviation.

results are presented in Fig. 5 in terms of the temporal mean and standard deviation. The results showed no sidewall effect and large fluctuations in bore celerity with the ratio of standard deviation to temporal mean U'/U_{mean} between 0.6 and 1.6 (Fig. 5). These large fluctuations might be related to the generation and advection of turbulent vortices in the roller as well as air bubble entrainment at the roller toe.

The instantaneous cross-sectional averaged celerity $\bar{U}$ was derived from the median perimeter data of the bore roller. The mean values are reported in Table 1, column 6. The instantaneous cross-sectional averaged celerity fluctuated rapidly with time about a median value. Yeh and Mok [20] reported fluctuations in bore celerity, although with lesser fluctuation magnitudes. The instantaneous celerity was not always positive, with negative celerity values consistent with intermittent backshifts of the instantaneous roller toe perimeter, seen for example in Fig. 1B, Inset about $t = 0.16$ and 0.24 s.

6. Conclusion and future work

In a breaking bore, the roller is associated with a sudden increase in water depth, a highly turbulent flow with large-scale vortical structures and strong turbulence interactions with the free surface. New unsteady experiments were conducted to investigate the upstream propagation of breaking bore roller. The roller toe propagation was a highly turbulent process. The toe perimeter shape fluctuated rapidly with transverse distance and time, and its transverse fluctuations were quantified in terms of the standard deviation $(X - X_{median})'/d_1 = 0.145$ at a given time. The characteristic transverse wave length of the toe perimeter was approximately 1.2 times the initial flow depth d_1. Both the standard deviation of toe perimeter location and characteristic transverse wave length were comparable to field observations in the Qiantang River bore (China). The data suggested the existence of streamwise coherent structures, in addition to the organised vortical motion in the shear layer.

The celerity of the roller toe fluctuated rapidly with time and space, although in a quasi-two-dimensional manner on average. The sidewalls had little effect on the upstream propagation of the roller within the laboratory flow conditions. The instantaneous longitudinal free-surface profile of the roller showed significant temporal and spatial fluctuations. For $Fr_1 < 2$, a gradual rise in free-surface was clearly seen in front of the roller, and both the roller toe elevation and its vertical fluctuations decreased with increasing Froude number.

While the bore propagation may be analysed in an integral form in first approximation, the present study showed that the propagation of breaking bore is a very turbulent process. The rapid fluctuations in roller toe perimeter and free-surface profiles indicate a strongly three-dimensional turbulent flow motion.

Acknowledgments

The authors acknowledge the financial supports of the Australian Research Council (Grant DP120100481) and Agence Nationale de la Recherche (Projet MASCARET 10-BLAN-0911-01), and the technical assistance of Jason Van Der Gevel and Matthews Stewart (The University of Queensland).

References

[1] R.A.R. Tricker, Bores, Breakers, Waves and Wakes, American Elsevier Publ. Co., New York, USA, 1965.
[2] J. Lighthill, Waves in Fluids, Cambridge University Press, Cambridge, UK, 1978, 504 p.
[3] H. Chanson, Tidal Bores, Aegir, Eagre, Mascaret, Pororoca: Theory and Observations, World Scientific, Singapore, 2011, 220 p. (ISBN 9789814335416).
[4] S.F. Greb, A.W. Archer, Soft-sediment deformation produced by tides in aMeizoseismic area, Turnagain Arm, Alaska, Geology 35 (5) (2007) 435–438.
[5] N. Khezri, H. Chanson, Sediment inception under breaking tidal bores, Mech. Res. Commun. 41 (2012) 49–53, http://dx.doi.org/10.1016/j.mechrescom.2012.02.010, 1 video movie.
[6] H. Tanaka, X.T. Nguyen, M. Umeda, R. Hirao, E. Pradjoko, A. Mano, K. Udo, Coastal and estuarine morphology changes induced by the 2011 Great East Japan Earthquake Tsunami, Coast. Eng. J. 54 (1) (2012), http://dx.doi.org/10.1142/S0578563412500106.
[7] P. Lubin, S. Glockner, H. Chanson, Numerical simulation of a weak breaking tidal bore, Mech. Res. Commun. 37 (1) (2010) 119–121, http://dx.doi.org/10.1016/j.mechrescom.2009.09.008.
[8] H.G. Hornung, C. Willert, S. Turner, The flow field downstream of a hydraulic jump, J. Fluid Mech. 287 (1995) 299–316.
[9] J.A. Liggett, Fluid Mechanics, McGraw-Hill, New York, USA, 1994.
[10] H. Chanson, Momentum considerations in hydraulic jumps and bores, J. Irrig. Drain. Eng. ASCE 138 (4) (2012) 382–385, http://dx.doi.org/10.1061/(ASCE)IR.1943-4774.0000409.
[11] J.W. Hoyt, R.H.J. Sellin, Hydraulic Jump as 'Mixing Layer', J. Hydraul. Eng. ASCE 115 (12) (1989) 1607–1614.
[12] D. Long, N. Rajaratnam, P.M. Steffler, P.R. Smy, Structure of flow in hydraulic jumps, J. Hydraul. Res. 29 (2) (1991) 207–218.
[13] L.P. Bernal, A. Roshko, Streamwise vortex structure in plane mixing layers, J. Fluid Mech. 170 (1986) 499–525.
[14] O. Levin, V.G. Chernoray, L. Lofdahl, D.S. Henningson, A study of Blasius wall jet, J. Fluid Mech. 539 (2005) 313–347.
[15] D. Mouaze, F. Murzyn, J.R. Chaplin, Free surface length scale estimation in hydraulic jumps, J. Fluids Eng. ASME 127 (2005) 1191–1193.
[16] Y. Chachereau, H. Chanson, Free-surface fluctuations and turbulence in hydraulic jumps, Exp. Thermal Fluid Sci. 35 (6) (2011) 896–909, http://dx.doi.org/10.1016/j.expthermflusci.2011.01.009.
[17] C. Koch, H. Chanson, Turbulence measurements in positive surges and bores, J. Hydraul. Res. 47 (1) (2009) 29–40, http://dx.doi.org/10.3826/jhr.2009.2954.
[18] N.J. Docherty, H. Chanson, Physical modelling of unsteady turbulence in breaking tidal bores, J. Hydraul. Eng. 138 (5) (2012) 412-419, http://dx.doi.org/10.1061/(ASCE)HY.1943-7900.0000542.
[19] Y.H. Toi, H. Chanson, Turbulent mixing in breaking tidal bores: comparison between field and laboratory data, Paper A10201, 10 p., in: Z. Wang, J.H.W. Lee, J. Gao, S. Cao (Eds.), Proc. 35th IAHR World Congress, 8–13 September, Chengdu, China, 2013.
[20] H.H. Yeh, K.M. Mok, On turbulence in bores, Phys. Fluids A A2 (5) (1990) 821–828.
[21] A. Valiani, Linear and angular momentum conservation in hydraulic jump, J. Hydraul. Res. 35 (3) (1997) 323–354.